JOURNAL OF MATERIALS SCIENCE 25 (1990) 3592–3604

Sliding friction of ceramics: mechanical action of the wear debris

J. DENAPE*
Ecole Nationale Supérieure des Mines, B.P. 87, F-91003 Evry Cedex, France
J. LAMON
Battelle-Geneva, 7, route de Drize, CH 1227 Carouge/Geneva, Switzerland

The wear behaviour of four commercially available structural ceramics (silicon carbide, SiAlON, alumina and partially stabilized zirconia) was investigated at room temperature, under various conditions of sliding friction using closed dry and open lubricated systems. Primary emphasis was placed on the mechanical action of wear debris. It was thus demonstrated that the circulation of wear debris in the sliding interface simultaneously controls the wear rate and the friction response. The parameters which control the accumulation or the elimination of wear debris were determined. The wear behaviour of the examined ceramics was found to be highly dependent upon the quantity of entrapped wear debris.

1. Introduction

Before the emergence of new materials such as polymers, composites and ceramics, structural applications were dominated by metals and alloys. This strongly influenced the approach to tribology which was dominated by the adhesion theory. Only recently the approaches to wear have considered the relationships between the different competing wear mechanisms [1, 2] which have been identified (abrasion, oxidation, delamination, melting, etc.). Of particular interest is the work by Suh and Sin [2], who considered the contribution of the wear particles as a component of the frictional force.

Comparatively little is known about the friction and wear of ceramics, which has been approached from the view of contact damage. Several studies [3–5] have examined the friction and wear of some structural ceramics when rubbed against a diamond indentor or using the pin-on-disc technique. Moreover, extensive work has concentrated on the surface fracture induced by Hertzian contact or Vickers indentation [6–12]. This surface fracture results from brittle mechanisms at the macroscopic level. It is usually characterized using macroscopic properties. The fracture models which have been developed have been applied to abrasive wear, where material is removed by chipping [13–15]. These failure models are restricted to sharp contacts. Therefore, they are not adequate for sliding friction and wear description. Moreover, a scale factor is involved because the wear particles which are observed in friction prove to be microscopic, far smaller than the grains of the ceramic microstructure [3, 5, 16, 17]. Therefore, the mechanisms responsible for friction wear fall outside the field of macroscopic failure.

In order to meet this scale requirement, the appropriate approach to friction wear must take into account the presence of debris circulating in the contact area. The important role of debris has been examined by Godet to explain the wear mechanisms observed in dry conditions with a vibrating frictional contact [18]. This so-called third body approach tries to rationalize the many aspects which are common to different types of materials in different types of rubbing contact. This is an important attempt to evaluate the tribological behaviour of materials.

In the third body approach, the wear mechanism is broken down into the following three stages, with their own kinetics, interacting to a high degree with the others [17].

1. The formation of the debris (e.g. the various mechanisms of material removal).
2. The evolution of debris in the contact area (e.g. the physical and chemical changes induced by grinding, oxidation).
3. The behaviour of the debris (e.g. removal from (open or lubricated systems) or accumulation (dry closed systems) in the contact interface). The debris entrapped in the sliding contact can separate the counteracting surfaces thus presenting load-carrying capacities exactly like a lubricant.

The present paper has a dual intent: first, to demonstrate that the presence of debris in the sliding interface of structural ceramics controls the wear behaviour and the friction response; second, to evaluate the wear behaviour of commercially available structural

Present address: Ecole Nationale d'Ingénieurs de Tarbes, Laboratoire de Génie de Production, Chemin d'Azereix, B.P. 1629, F-65016 Tarbes, France.

0022–2461/90 $03.00 + .12

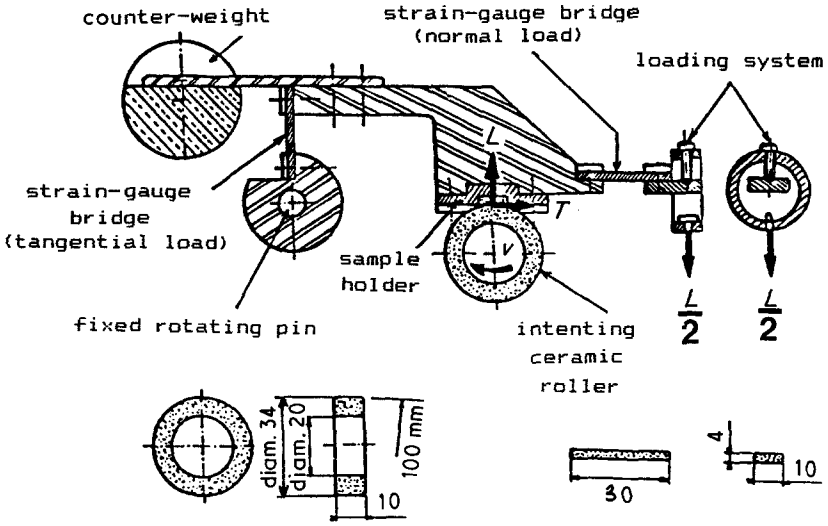

Figure 1 Sketch of the roller-on-beam tribometer.

ceramics in sliding friction conditions involving or not the contribution of wear debris.

2. Experimental procedure

Two types of friction experiments were selected, on the basis that they favour either the accumulation or the elimination of the wear debris: dry conditions for entrapping particles in the sliding interface, and lubricated conditions for enhancing the escape of wear debris. The former case focuses on the dynamic role of debris, whereas the latter favours debris formation.

The first series of experiments was conducted on a roller-on-beam tribometer which was designed for dry friction tests at room temperature and low loads. This tribometer rotates a ceramic roller (referred to as the indenting roller) against a flat beam of the same ceramic (Fig. 1). Dead loads are applied through an arm equipped with two strain gauge bridges allowing continuous recording of the friction force, F, thus giving the friction coefficient, μ. The test programme first applied constant loads ranging between 2 and 40 N at a constant sliding speed of 0.25 m sec^{-1}, and then sliding speeds ranging between 0.1 and 4 m sec^{-1} at a constant load of 5 N. The total duration of tests corresponded to slid distances of 4000 m. Several specimens were used per test condition.

Experiments were also conducted under distilled water, with the purpose of eliminating debris from the sliding interface.

The second series of friction experiments was conducted on a roller-on-roller tribometer for lubricated tests under heavy loads at room temperature. This tribometer rotates a ceramic roller (referred to as the indenting roller) against an identical roller counterface of the same ceramic (Fig. 2). The same rollers as previously were used. The test programme followed a standard procedure employed by the automotive industry. The load was initially increased up to 1000 N in steps of 200 N, both rollers rotating at 3000 r.p.m. (rolling contact). The relative speed of one roller was then gradually increased from 0 to 3.8 m sec^{-1} over 30 min, at the constant load of 1000 N (sliding contact). The friction coefficient was derived from the measurement of friction torque. Mineral oil was used as lubricating fluid. The role of the lubricant was to ensure hydrodynamic load carrying, and removal of all the debris. These testing conditions therefore allowed debris formation and the wear behaviour in the absence of debris to be examined.

In order to generate well-defined curved-on-flat contacts, the outer surface of the indenting rollers had a transverse curvature radius of 100 mm. Elliptical

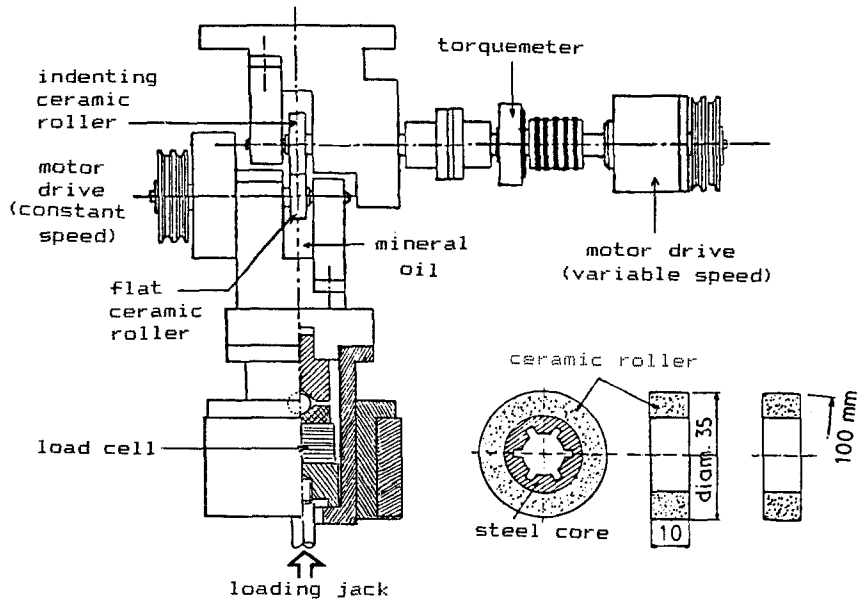

Figure 2 Sketch of the roller-on-roller tribometer.

TABLE I Main properties of the tested ceramics

Material	Density	Grain size (μm)	Elastic modulus (GPa)	Hardness (GPa)	Fracture toughness (MPa $m^{1/2}$)	Poisson's ratio
SSC*	3.14	3–8	410	29	3.5	0.16
SiAlON*	3.20	1–5	300	16	4.8	0.26
PSZ†	5.7	40–50	200	11	7	0.29
Al_2O_3†	3.9	2–5	240	13	3.5	0.25

*"Céramiques et Composites" Co., France.
†"Desmarquest" Co., France.

and circumferential tracks were obtained on the surfaces of the beams and of the flat rollers, respectively. The volume, V, of removed material was satisfactorily derived from the wear-track dimensions using the following equations

$$V = \frac{\pi}{2} abh \text{ (beams)} \quad (1)$$

$$V = \pi dlh \text{ (flat rollers)} \quad (2)$$

where $2a$ and $2b$ are, respectively, the long and small axes of the ellipse, h is the depth of the wear tracks, d the diameter of the flat roller and l the track width. These dimensions were measured using a profilometer, the test being stopped at predetermined sliding distances.

Four ceramics covering a broad spectrum of the family of structural ceramics were selected for this study: i.e. sintered silicon carbide (SSC), sintered silicon nitride of the SiAlON family (SiAlON), partially stabilized zirconia (PSZ) and alumina (Al_2O_3). Their main properties are summarized in Table I.

The surface finish was characterized prior to testing by roughness, R_a, which was measured in the transverse direction in terms of the mean height of irregularities. The surface of the indenting rollers was as-ground (R_a between 0.5 and 1 μm) whereas the surfaces of the beams and the flat rollers had been smoothly polished: R_a was between 0.02 and 0.05 μm for the beams, and smaller than 0.1 μm for the rollers. Before testing, the surfaces of beams and rollers were carefully cleaned, in order to eliminate the impurities which could affect the wear behaviour of the materials and the reproducibility of the results.

3. Results

3.1. Dry friction tests

Fig. 3 shows an example of the typical wear curves which were obtained. Wear is expressed in terms of the volume of material removal. It can be seen that after

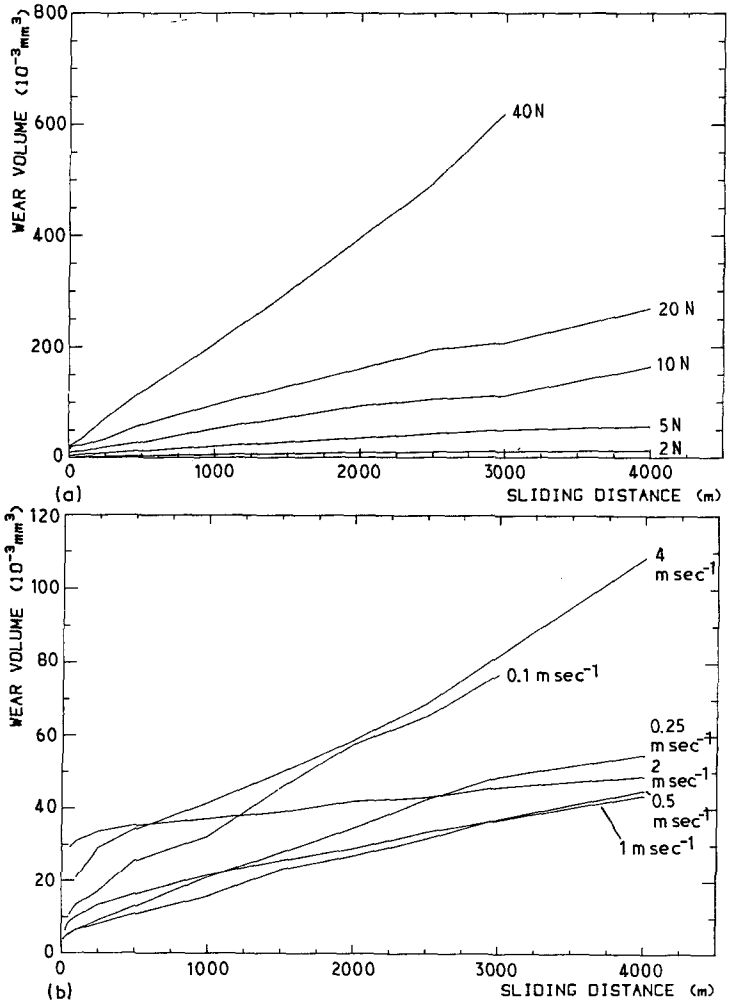

Figure 3 Volumes of material removal plotted against sliding distance for SSC, at various loads and a constant speed of 0.25 m sec^{-1} (a) and at various sliding speeds and a constant load of 5 N (b).

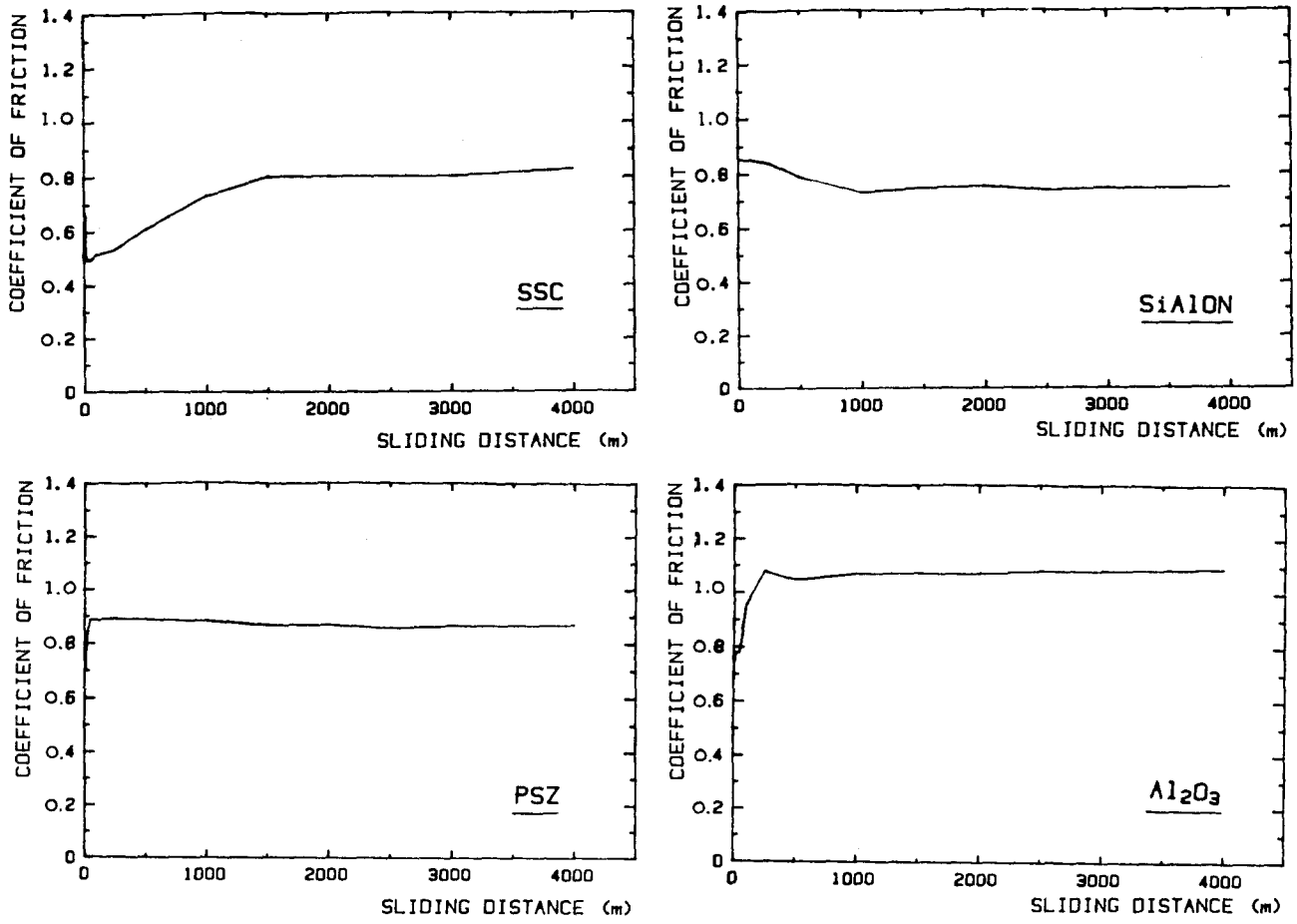

Figure 4 Variations of coefficient of friction with sliding distance (applied load 5 N, sliding speed 0.25 m sec^{-1}).

the short initial running-in period, wear exhibited a constant rate phase.

For an easy comparison of the wear results, the measured volume of material removal in the steady-state phase was converted to a normalized wear rate, W, according to

$$W = \frac{V}{LD} \tag{3}$$

where W is the wear rate ($mm^3 N^{-1} m^{-1}$), V the volume of removed material (mm^3), L the applied load (N) and D the total distance slid (m).

3.1.1. Wear rates

The wear rates, W, were calculated from the measured volumes of material removed by linear regression analysis. The wear rates exhibit a more or less significant scatter although they were obtained on identical specimens. As discussed below, it seems logical to relate this scatter to the production of wear debris.

The wear rate is mainly dependent upon the material, and upon the sliding speed. The highest wear was observed on PSZ followed by SiAlON (wear rate up to 50 to 100 $\times$ 10^{-6} $mm^3 N^{-1} m^{-1}$), whereas SSC and alumina experienced comparatively low wear (2 to 5 $\times$ 10^{-6} $mm^3 N^{-1} m^{-1}$ wear rate).

These results are an order of magnitude lower than pin-on-disc data reported in the literature for silicon carbide and silicon nitride [3] and for polycrystalline alumina [20]. They are comparable to the values obtained in a number of recent wear studies of ceramics tested in reciprocal wear tests [20, 21]. The above difference may be logically attributed to the contact configuration, which was less sharp in the present study than in pin-on-disc tribometers.

3.1.2. Friction coefficients

Fig. 4 shows typical plots of friction coefficients obtained in identical nominal conditions. The variation of coefficients of friction with distance (or time) of sliding may be summarized by using the three typical plots shown by Fig. 5. The important point to note from the figures is that the friction behaviour of these materials is not characterized by a single value of the friction coefficient: but instead a steady-state value, μ_s, is reached after a certain slid distance depending upon the material.

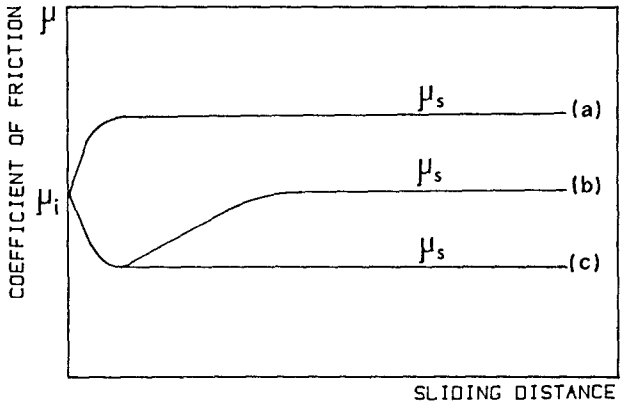

Figure 5 Coefficient of friction plotted against sliding distance: (a) for PSZ, Al_2O_3, and SiAlON at high speed; (b) for SSC; (c) for SiAlON at low speed.

The steady-state friction coefficient, μ_s, generally results from a rather rapid increase of the friction coefficient, except for SSC where an initial slow decrease occurred first. SiAlON was a special case at low sliding speed because the friction coefficient decreased to a low value of μ_s.

μ_s exhibits a significant dependence on the sliding speeds. The μ_s values lie in the range 0.5 to 1.10. Alumina generally gives the highest friction coefficient, followed by PSZ, SiAlON and SSC. These data are logically larger than the pin-on-disc data reported in the literature, which lie in the range 0.2 to 0.7 [3–5].

3.1.3. Influence of the applied load at constant sliding speed

The applied load does not exert a significant influence on the friction coefficient (Fig. 6a). In contrast, apart from SSC where the wear rate was roughly constant,

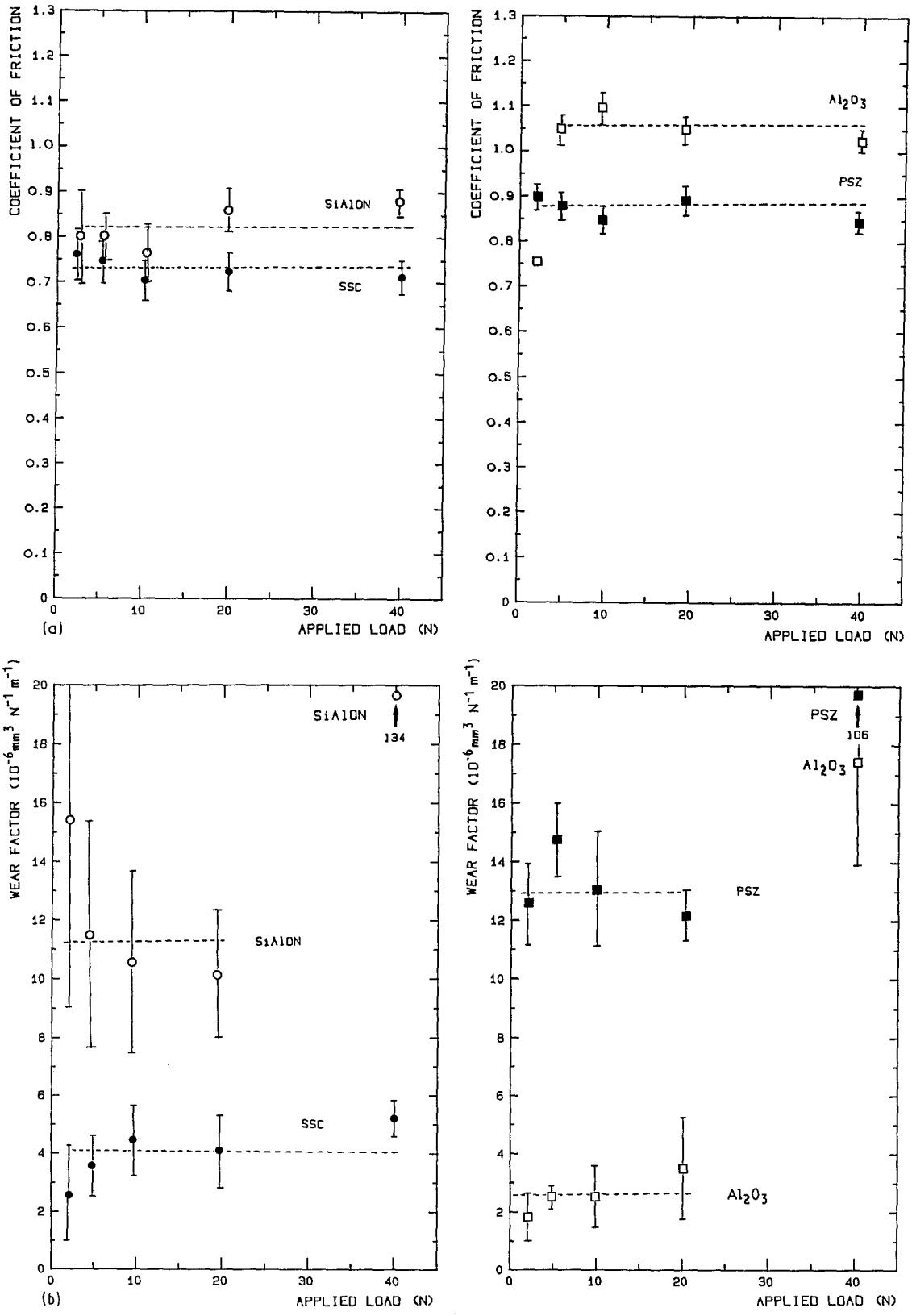

Figure 6 Plots of (a) coefficient of friction and (b) wear rate as a function of the applied load (sliding speed 0.25 m sec^{-1}).

SiAlON, PSZ and to a lesser extent Al_2O_3 showed an accelerated regime at increasing loads (Fig. 6b). This wear acceleration did not affect the steady-state friction coefficient. This clearly indicates that the load controls the material removal process and particularly the formation of wear debris. However, it does not control the interaction of the sliding surfaces which is characterized by the friction coefficient.

3.1.4. Influence of the sliding speed at constant load

Plots of the wear rate and the friction coefficient, μ_s, against the sliding speed (Fig. 7) reveal fundamental features, and highlight the dynamic aspect of the problem. First, the wear rate and the friction coefficient always exhibit opposite changes with increasing sliding speed. Second, there is a critical sliding speed leading

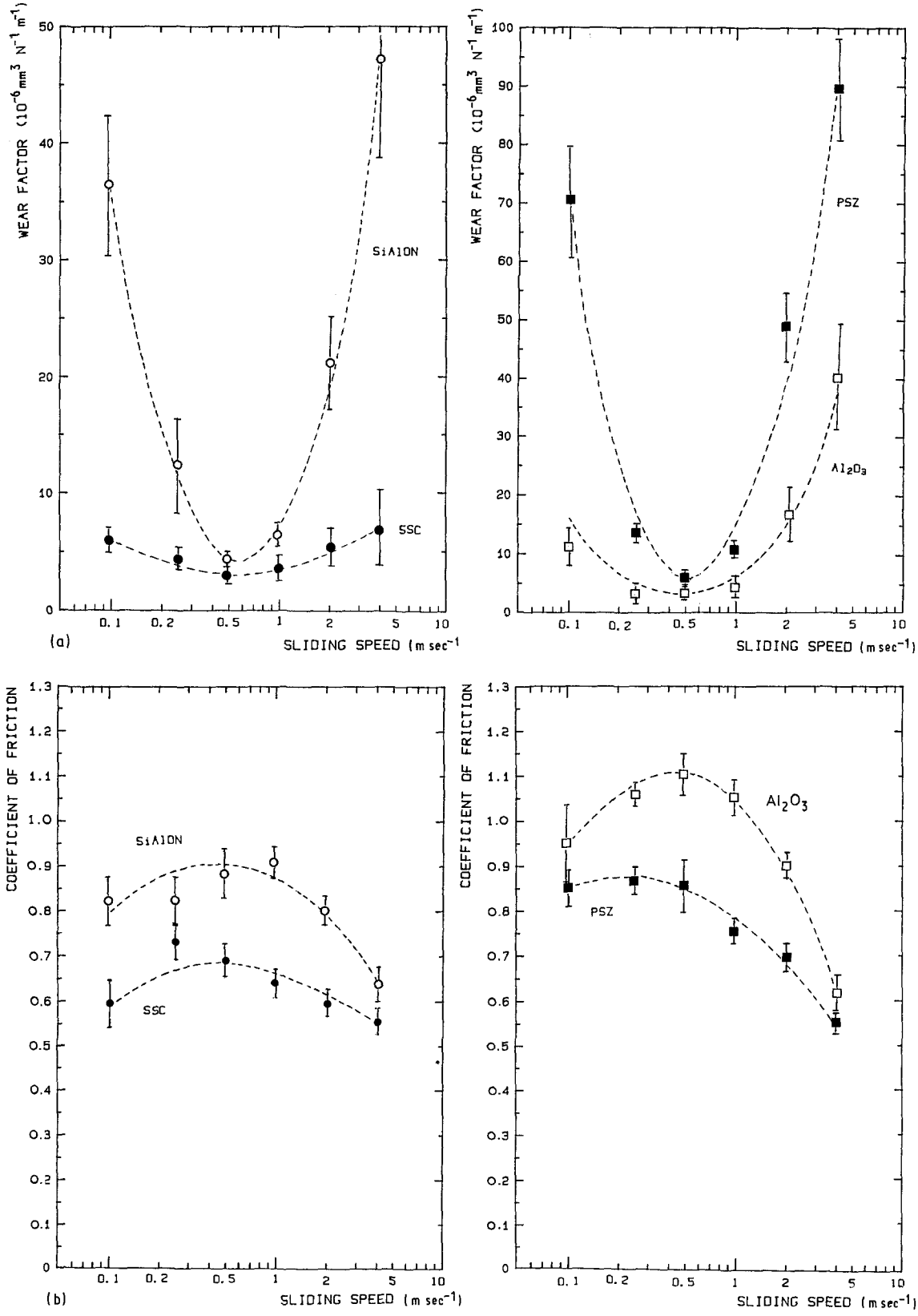

Figure 7 Variations of (a) wear rate and (b) coefficient of friction with sliding speed (applied load 5 N).

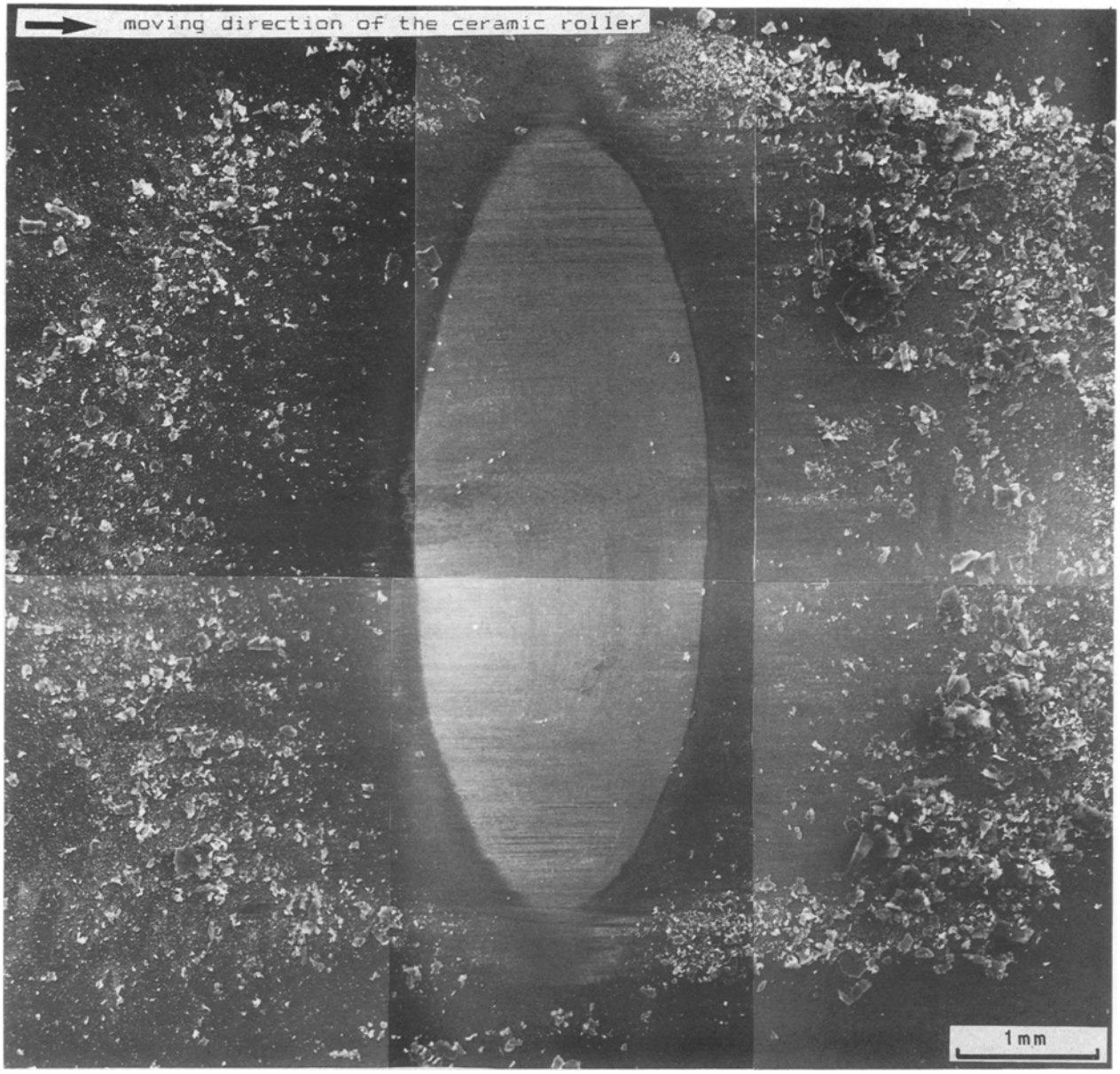

Figure 8 Optical micrograph of a friction track of SSC (applied load 40 N, sliding speed 0.25 m sec^{-1}, sliding distance 500 m) showing wear debris.

to a minimum wear rate and a maximum steady-state friction coefficient. This critical speed is about 0.5 m sec^{-1} for all four ceramics. At increasing sliding speeds, below the critical speed the wear rate decreases, and then increases beyond it. The opposite trend is observed with the friction coefficient.

The sliding speed is thus a preponderant factor which controls the friction coefficient, and the wear rate. At first sight, paradoxically the maximum wear rate corresponds to a minimum friction coefficient whereas maximum friction coefficient causes minimum wear rate.

In the present conditions of dry friction, SSC exhibited the most favourable wear characteristics: the lowest friction coefficient, the lowest wear rates, and the lowest sensitivity to sliding speed.

3.1.5. Observation of the wear tracks

Microscopic examination of the friction tracks revealed the presence of important quantities of debris within but also outside the wear track (Fig. 8). The debris was present at both entry and exit of the track, indicating that it is eliminated from the sliding interface or recycled.

Finer debris was observed within the friction tracks. It was always a whitish colour, regardless of the material. Two types of debris were identified: free individual rounded particles, with a size of 0.1 to 0.5 μm (Fig. 9a), and more or less dense agglomerates forming flakes (SSC, Fig. 9b) or platelets (PSZ, Fig. 9c). Further examination of the worn surfaces for identification of the damage mechanisms required removal of the layers of debris which masked the subjacent material.

The worn surface of SSC appeared smoothly polished (Fig. 10a) with porosity filled in by very fine debris. Abrasion grooves and micro-chipping were observed at higher loads (Fig. 10b).

Al_2O_3 exhibited pulled-out grains, at all loads and speeds. These torn-off grains were finely ground and accumulated in small dense films adherent to the worn surface (Fig. 10c).

SiAlON showed large grooves at low loads and speeds (Fig. 10d). Wear proceeded by an abrasion

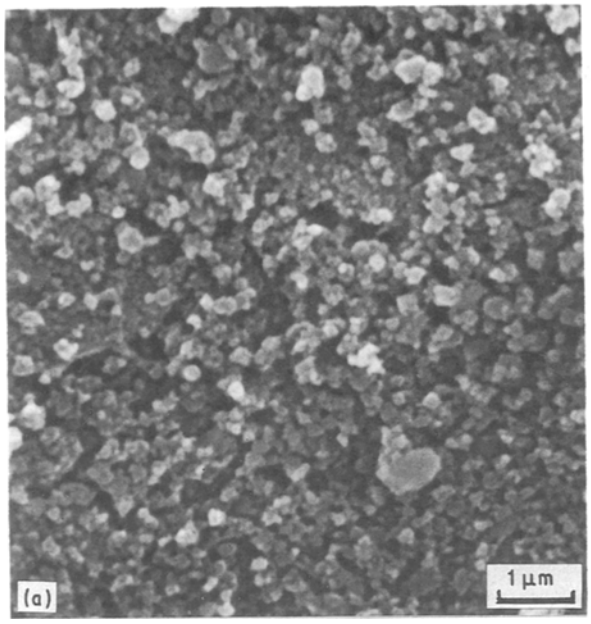

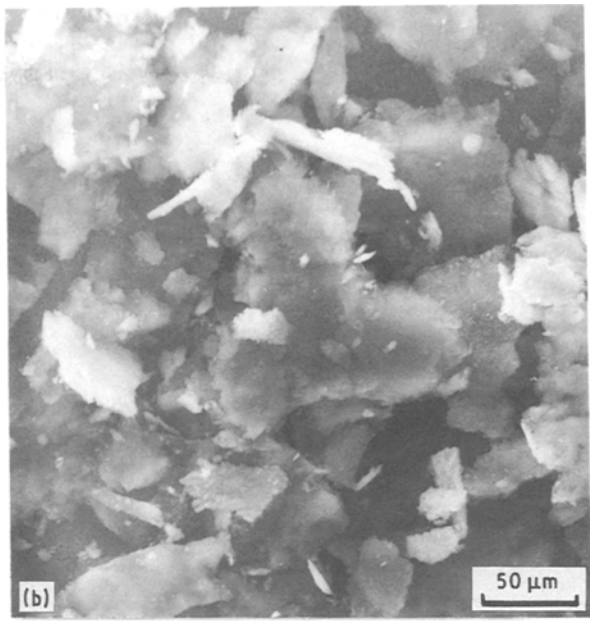

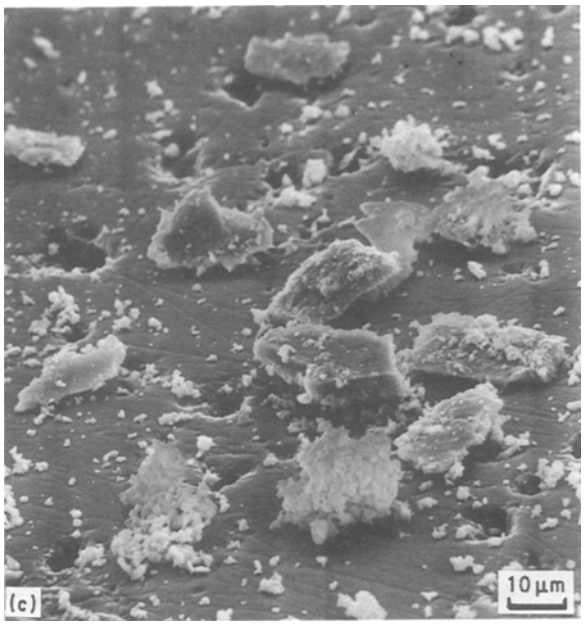

Figure 9 Electron micrographs of various wear debris (sliding speed 0.25 m sec^{-1}): (a) free individual particles (SiAlON, load 2 N); (b) agglomerates forming flakes (SSC, load 40 N); (c) dense agglomerates forming platelets (PSZ, load 5 N).

mechanism involving large accumulations of fine debris adherent to pores and probably also larger particles dragged within the sliding interface. At high loads and speeds, particle removal and debris accumulation occurred by the same mechanism as for alumina (Fig. 10e).

With PSZ, debris was gathered in large dense films adherent to the surface (Fig. 10f).

The examination of the worn surfaces has thus allowed the presence of particles or accumulation of particles to be detected. The debris contributed to the wear process through the following mechanisms:

(a) polishing involving fine individual particles, circulating along the sliding contact (SSC);

(b) abrasion by larger particles or accumulations trapped (SiAlON) or not (SSC) in pores;

(c) tearing-off or pulling-out of grains associated with the accumulation of fine debris in dense films adherent to the worn surface (Al_2O_3, SiAlON, PSZ).

3.2. Friction tests in the presence of distilled water

Tests under distilled water on the same tribometer induced significant changes in the wear behaviour. All four ceramics gave a drop in the steady-state friction coefficient, which was significant for SSC, SiAlON and Al_2O_3, and slight for PSZ (Table II). In parallel, apart from SiAlON where wear rates were less important than in dry friction, they all exhibited marked wear rate increases (Fig. 11). PSZ experienced very severe wear (up to 200×10^{-6} mm^3 N^{-1} m^{-1} wear rate) when compared with SSC, Al_2O_3 and SiAlON. SiAlON and Al_2O_3 exhibited wear rates decreasing to a constant value which was reached after a short sliding distance for SiAlON and a long one for Al_2O_3. This explains why wear was less severe for SiAlON and more severe for Al_2O_3, than in dry friction.

Microscopic examination of the wear tracks confirmed that the debris had been completely eliminated from the sliding interface (Fig. 12), except for PSZ and to a lesser extent for SiAlON. Residual accumulations of particles were observed on PSZ (Fig. 12a) whereas the pores of SiAlON were filled by very fine debris (Fig. 12b). This induced important changes in the wear mechanisms. Except PSZ, all the ceramics exhibited smooth surfaces, i.e. polished surfaces (SSC and

TABLE II Steady-state friction coefficients (applied loads 5 N, sliding speeds 0.5 m sec^{-1})

Conditions	μ_s			
	SSC	SiAlON	PSZ	Al_2O_3
Dry tests	0.69	0.90	0.86	1.10
Tests in distilled water	0.30	0.45	0.80	0.25

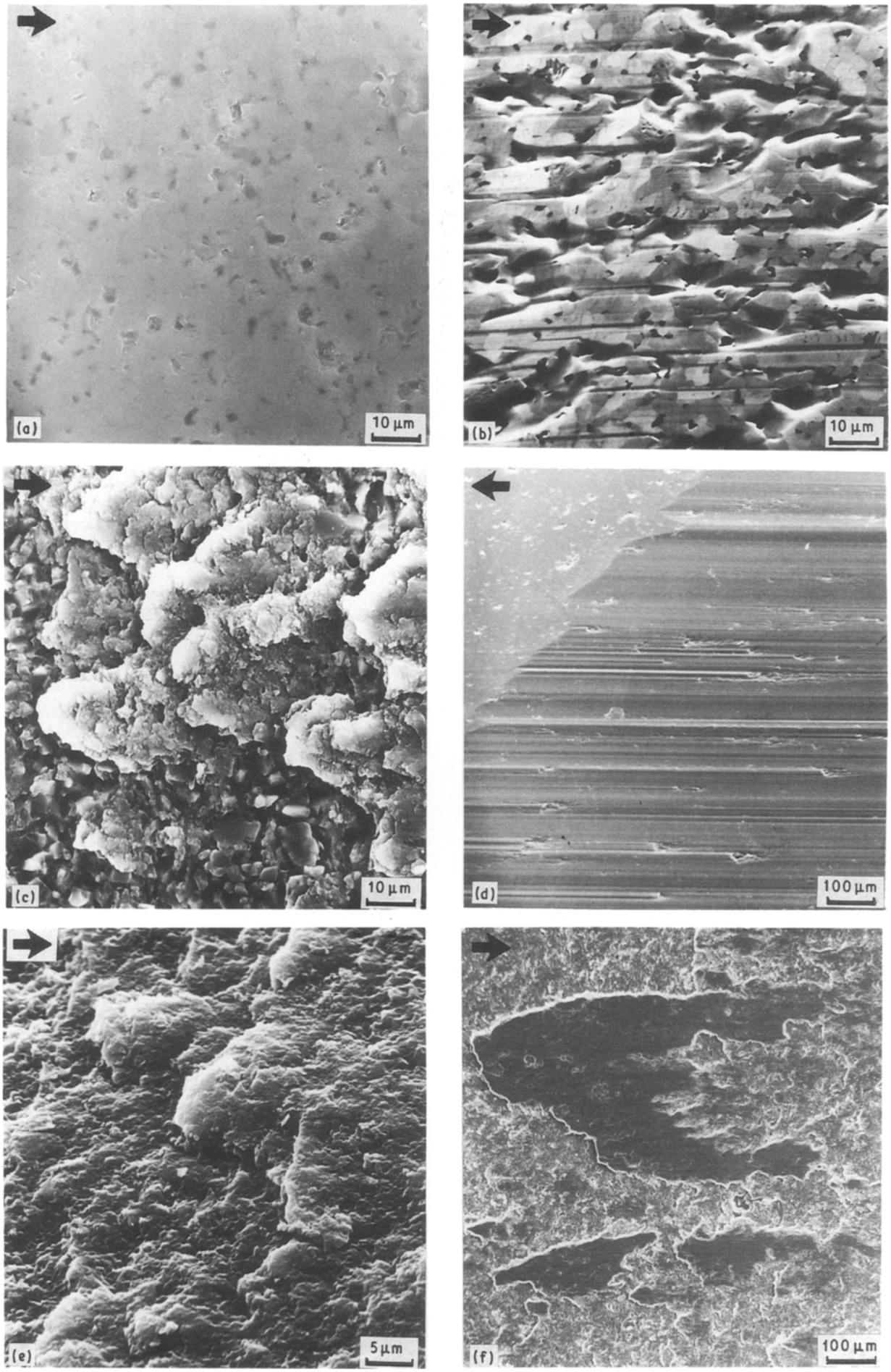

Figure 10 Electron micrographs of worn surfaces after dry friction tests (sliding speed 0.25 m sec^{-1}, sliding distance 4000 m) showing various wear mechanisms. (a) Polishing of SSC (applied load 5 N); (b) abrasion and microchipping (SSC, load 20 N); (c) grain removal and debris accumulation (alumina, load 40 N, sliding distance 1000 m); (d) abrasion (SiAlON, load 5 N); (e) particle removal and debris accumulation (SiAlON, load 40 N); (f) particle removal and dense films of debris (PSZ, load 5 N).

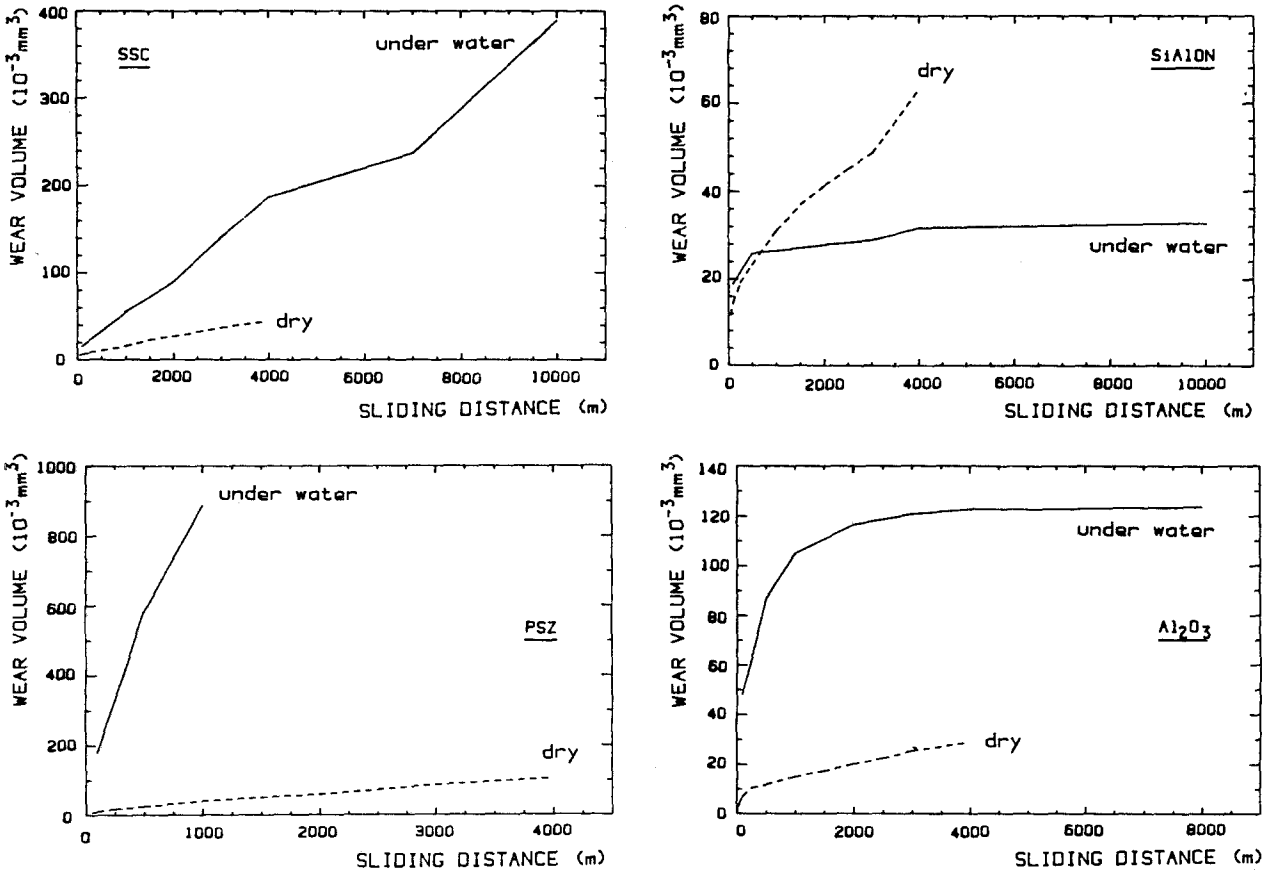

Figure 11 Influence of distilled water on wear volumes plotted as a function of the sliding distance (the dotted lines show the wear volumes measured under dry friction conditions).

Al_2O_3: Figs 12c and d), and mirror finish surfaces (SiAlON: Fig. 12b). The worn surface of PSZ was less irregular than in dry friction tests (Fig. 12a). Moreover, it is worth noting that a few short cracks approximately perpendicular to the sliding direction, as well as microchipping in the vicinity of pores (Fig. 12c) were observed in SSC.

3.3. Lubricated tests

A different trend was again observed under lubricated conditions and high loads with the roller-on-roller tribometer. SiAlON and PSZ experienced low wear, whereas SSC and Al_2O_3 exhibited poor wear behaviour (Table III). In particular the surface of the Al_2O_3 rollers was so degraded before the sliding conditions were reached that wear data could not be measured.

Significant decreases in the friction coefficient were observed when compared with dry friction data. However, the friction coefficient of SSC is comparable to that one obtained under distilled water, which indicates that the current lubricant did not present a load-carrying effect. The high wear rate can be logically attributed to the resulting high applied loads.

For SiAlON and PSZ, the friction coefficient is significantly lower than under distilled water, which reflects the load-carrying effect of the lubricant. This effect is also substantiated by the low wear rate which was observed.

Microscopic observation of the wear tracks confirmed that all the debris was removed from the sliding interface. The following mechanisms have been identified: polishing for SiAlON and PSZ; microchipping for SSC and for PSZ; grain fracture for Al_2O_3.

4. Discussion: action of debris and wear process

4.1. Tests under distilled water

The results obtained under distilled water demonstrate that, as observed by several authors [22, 23], when wear particles are removed from the sliding interface, the coefficient of friction decreases to a low value. The surface polishing which is responsible for this low value may be attributed to circulation of the fine individual particles being eliminated from the interface. The friction coefficient decreases reflect the component of the frictional force acting in dry conditions, induced by abrasion by wear particles and debris agglomerates. PSZ for which agglomerates of debris were still present in the sliding interface did not show a marked decrease in the friction coefficient.

Results under distilled water also showed that the elimination of debris causes wear rate increases. This indicates that the wear particles present load-carrying capacities. The cracks which were observed at the surface of SSC reflect the high loads operating in the absence of debris.

SiAlON is an interesting case, as it experienced less

TABLE III Wear rates and steady-state friction coefficients obtained on the roller tribometer at high loads (1000 N) and lubricated conditions

Material	Wear rate (10^{-6} mm^3 N^{-1} m^{-1})	Friction coefficient
SSC	> 100	0.2 –0.45
SiAlON	0.1	0.11
PSZ	5	0.06–0.14
Al_2O_3	–	–

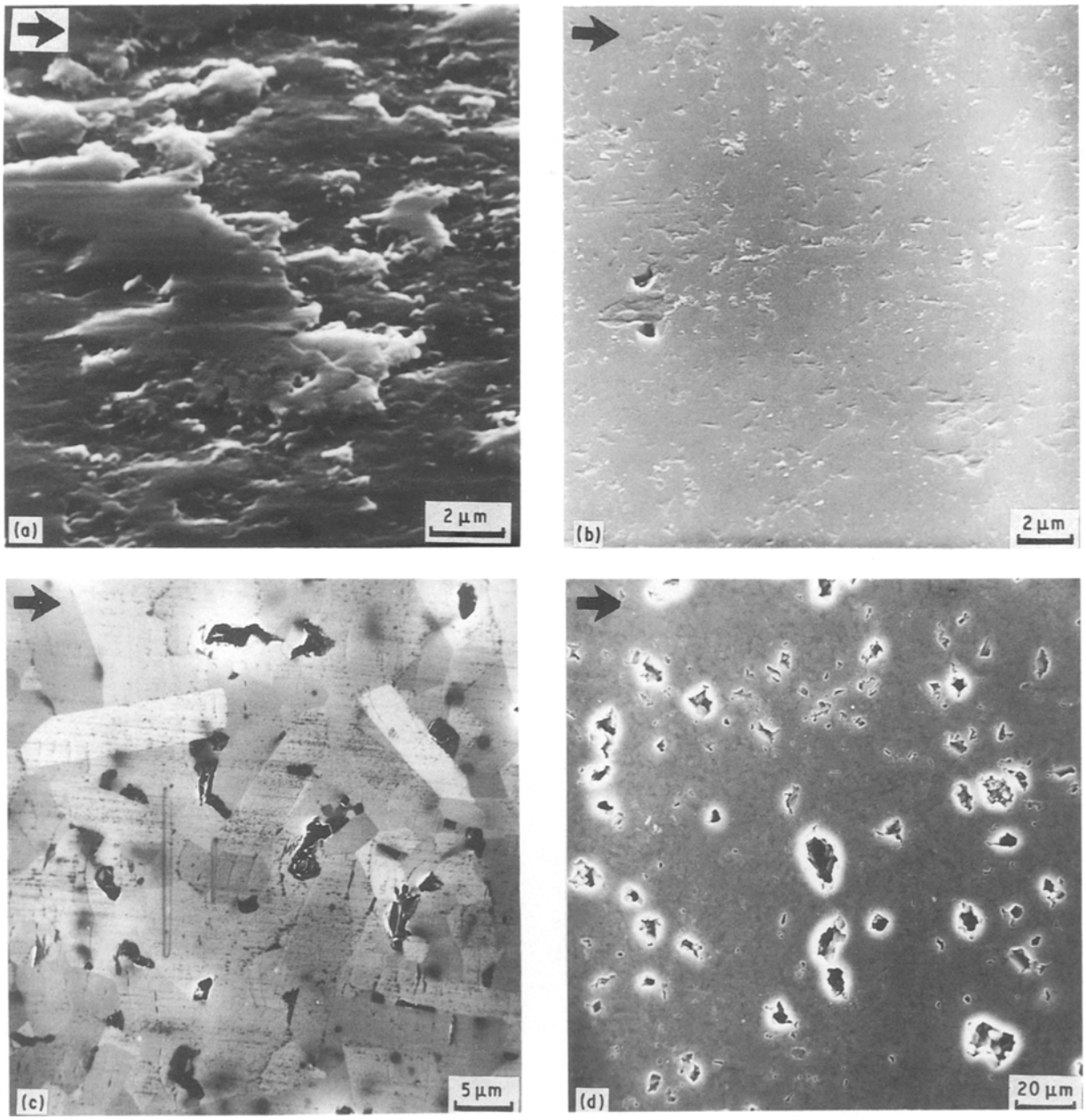

Figure 12 Electron micrographs of worn surfaces after wear tests under distilled water (applied load 5 N, sliding speed 0.25 m sec^{-1}) showing the following phenomena: (a) accumulation of debris (PSZ, sliding distance 1000 m); (b) polishing with filling in of pores (SiAlON, sliding distance: 10 000 m); (c) anisotropic wear of grains (SSC, sliding distance 10 000 m); (d) polishing (alumina, sliding distance 6000 m).

important wear than in dry conditions, as a result of rapid wear decrease to a low constant rate. This trend which was also observed on alumina but over a much longer sliding distance may be attributed to the surface adaptation phenomenon involving finely polished sliding surfaces. As a consequence, the real contact area is comparable to the apparent one which induces a uniform distribution of low pressions. However, one should also consider the possible load-carrying capacity of distilled water, suggesting that SiAlON presents favourable wetting properties. This point however, requires further consideration.

4.2. Lubricated tests: debris formation

The results obtained under lubricated conditions also confirm that the elimination of debris decreases the friction coefficient. In the absence of wear debris, material removal proceeds by polishing at low loads and cracking at higher loads. The transition between both mechanisms depends on the material. As shown by the friction tracks, SiAlON exhibited the highest resistance to cracking followed by PSZ, SSC and finally Al_2O_3. It is interesting to observe that this ranking is consistent with the fracture toughness data, except for PSZ which showed microcracking despite a higher fracture toughness than SiAlON. On PSZ testing, combustion of the oil film occurred at a sliding speed of about 2.5 m sec^{-1} as a result of the low thermal conductivity of PSZ which induced elevated temperatures. Since the load-carrying capacity of the lubricant was no longer operating, PSZ was subjected to higher loads than SiAlON, which may explain why PSZ exhibited microcracking and higher wear than SiAlON. Further detailed analysis of the microchipping process should allow the exact relationships between wear resistance and fracture toughness to be established.

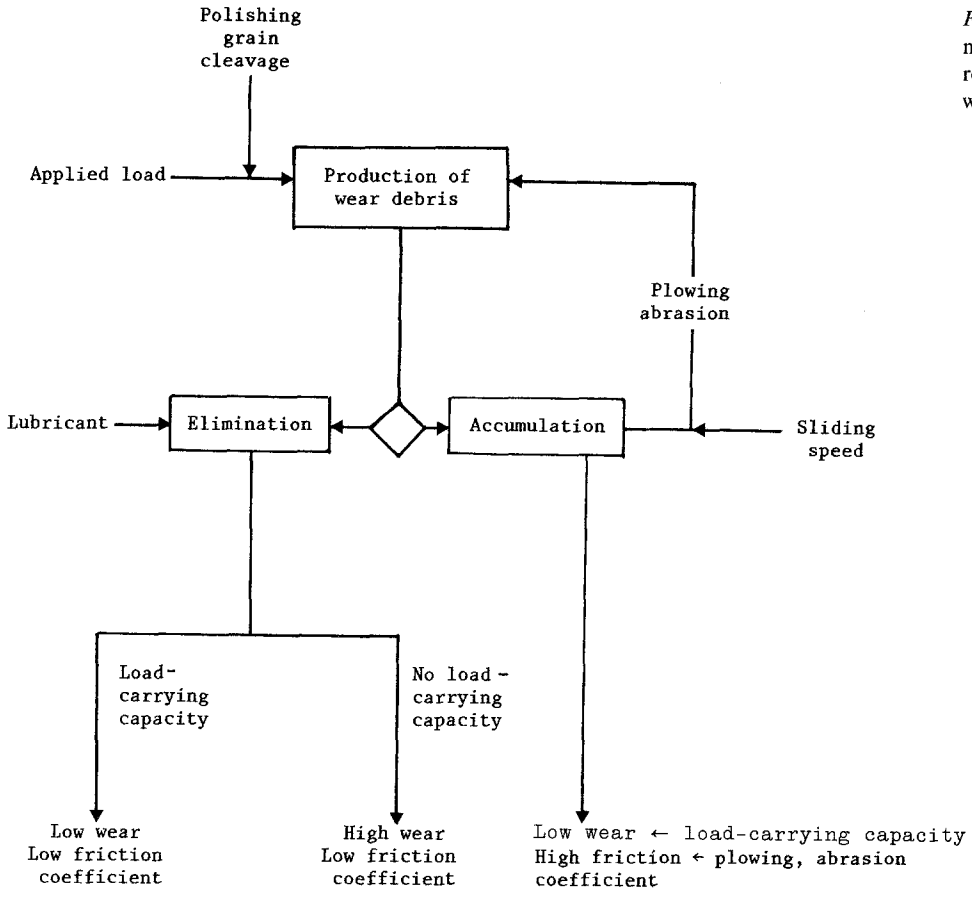

Figure 13 Diagram showing the main mechanisms of wear and the role played by debris in the friction wear of ceramics.

4.3. Influence of wear debris

The wear processes are described by Fig. 13. The fundamental phenomenon which determines the wear behaviour of ceramics may be summarized as follows: when the wear debris is removed from the sliding interface, the friction coefficient decreases to a low value and the wear rate correspondingly increases. This implies that when wear debris is accumulated in the sliding interface, the friction coefficient increases and the wear rate decreases. The wear debris has a dual action:

(a) it interacts with the sliding surfaces by plowing and abrasion, which increases the friction coefficient;

(b) it presents load-carrying capacity, which decreases the wear rate.

Variations in the friction coefficient reflect the evolution of the quantity of debris in the sliding interface and the dynamic equilibrium between production and elimination from the wear track. Stability of the friction coefficient corresponds to a constant quantity of debris; increases indicate a debris build-up phase whereas reductions reflect an elimination phase.

It was observed that at constant sliding speed, the steady-state friction coefficient is invariant, which indicates that constant quantities of debris are entrapped in the sliding interface. It appeared that the friction coefficient is independent of the applied load, which shows that the circulation of debris is controlled exclusively by the sliding speed.

Friction coefficient variations thus allow the influence of sliding speed on the wear rate to be explained. Below the critical speed, increasing speeds caused friction coefficient increases, indicative of a debris accumulation phase. The corresponding decrease in the wear rate confirms that the load-carrying effect of debris increases with the quantity of particles. Beyond the critical speed, friction coefficient drop indicates a debris elimination phase. As a consequence, the load-carrying effect of debris decreases, leading to the wear rate increases which have been observed.

The critical sliding speed provides the maximum friction coefficient, and therefore the maximum quantity of particles entrapped in the sliding interface. As a consequence, the wear rate was minimum as a result of a maximum load-carrying effect. The critical speed marks the limit between both phases of debris accumulation and elimination. This is a characteristic of the contact interface: it is logically independent of the ceramic.

Friction coefficient changes with sliding distance shown in Fig. 5 reflect the circulation of debris during friction tests. They show that in most cases (Al_2O_3, PSZ and SiAlON at high speed) the debris accumulates to a maximum constant quantity characterized by the steady state friction coefficient, μ_s. This behaviour is substantiated by the presence of layers of debris adherent to the sliding interfaces.

The initial decrease of the SSC friction coefficient indicates that an elimination phase occurred prior to accumulation of debris. This behaviour may be related to the production of the very fine debris which was observed on the sliding interface. This suggests that the accumulation of this very fine debris requires that a sufficient quantity is produced in a first step.

SiAlON exhibited a specific response at low speed, because the friction coefficient dropped to a low steady-state value. This indicates that the debris

was eliminated from the sliding interface. This phenomenon has not yet been elucidated.

Al_2O_3 exhibited the highest steady state friction coefficient, which is in relation to the large debris produced by grain pull-out.

SSC exhibited the lowest steady state friction coefficient, which may be attributed to the presence of very fine debris and the absence of debris layers in the sliding interface.

5. Conclusions

The wear behaviour of four commercial ceramics representing a broad spectrum of available structural ceramics has been investigated, with the intent to examine the influence of wear debris on the friction and wear behaviour. For this purpose, three different testing conditions were selected involving either the accumulation of the wear debris or its elimination from the sliding interface.

The wear sensitivity of the examined ceramics depends heavily on the testing conditions. In dry conditions involving the contribution of the wear debris entrapped in the sliding interface, SSC and Al_2O_3 gave the highest wear resistance, followed by SiAlON and PSZ. This trend is strongly affected by the elimination of debris, and completely reversed with a lubricant having load-carrying capacity: in lubricated conditions SiAlON showed the highest wear resistance followed by PSZ, SSC and Al_2O_3.

The debris determines the wear mechanism:

(a) Polishing is due to fine individual wear particles smaller than 1 μm, circulating in the sliding interface.

(b) Abrasion and grain pull-out are associated with dense accumulations of particles adherent to the sliding surfaces.

The fine individual debris has a dual action:

(a) it acts as a lubricant with a load-carrying effect, forming layers separating the sliding surfaces,

(b) it contributes to material removal by polishing.

The aggressive or protective action of fine debris depends essentially on the quantity entrapped in the sliding contact.

The circulation of wear particles in the sliding interface is reflected by the friction coefficient, which increases when particles are accumulated and decreases when particles are removed from the sliding interface. The accumulation and the elimination of debris are governed by the sliding speed. Regardless of the material, a critical sliding speed provides the maximum quantity of wear debris in the sliding interface, which induces a maximum friction coefficient and a minimum wear rate.

SiAlON exhibited specific features, such as a very important sensitivity to the presence of particles which strongly degraded the surface by abrasion. Moreover it showed a specific behaviour in lubricated conditions, and some favourable wetting properties.

The results of this study are in correlation with the principles of the third body theory. Therefore, this shows that sliding friction should not be approached exclusively from the material side, but rather through an overall framework into which the individual observations can be fitted. This should be an important step towards a unifying theory of wear.

References

1. S. C. LIM and M. F. ASHBY, *Acta Metall.* **35** (1987) 1.
2. N. P. SUH and M. C. SIN, *Wear* **69** (1981) 91.
3. D. C. CRAMMER, *J. Mater. Sci.* **20** (1985) 2029.
4. H. ARBABI and T. S. EYRE, *Metals Mater.* October (1986) 625.
5. O. O. ADEWOYE and T. F. PAGE, *Wear* **70** (1981) 37.
6. B. R. LAWN and T. R. WILSHAW, *J. Mater. Sci.* **10** (1975) 1049.
7. A. G. EVANS and T. R. WILSHAW, *Acta Metall.* **24** (1976) 939.
8. B. R. LAWN and M. V. SWAIN, *J. Mater. Sci.* **10** (1975) 113.
9. J. T. HAGAN, *ibid.* **14** (1979) 2975.
10. B. R. LAWN and A. G. EVANS, *ibid.* **12** (1977) 2195.
11. B. R. LAWN, A. B. EVANS and D. B. MARSHALL, *J. Amer. Ceram. Soc.* **63** (1980) 574.
12. D. B. MARSHALL, B. R. LAWN and A. G. EVANS, *ibid.* **65** (1982) 561.
13. D. B. MARSHALL, "Progress in Nitrogen Ceramics", Vol. 65 edited by F. L. Riley (Nijhoff, The Hague, 1983) pp. 635–56.
14. B. R. LAWN, S. M. WIDERHORN and D. E. ROBERTS, *J. Mater. Sci.* **19** (1984) 2561.
15. M. A. MOORE and F. S. KING, *Wear* **60** (1980) 123.
16. S. B. TOH and R. McPHERSON, Institute of Physics Conference Series, 75 (1986) 865.
17. E. BREVAL, J. BREZNAK and N. H. MacMILLAN, *J. Mater. Sci.* **21** (1986) 931.
18. M. GODET, *Wear* **100** (1984) 437.
19. Y. BERTHIER, C. COLOMBIE, M. GODET, G. LOFFICIAL and L. VINCENT, Eurotrib '85, Vol. II, edited by Soc. Fr. Tribologie (Elsevier, Amsterdam, 1985) Section 5.5.1.
20. M. YOUSEFFI and R. FREER, *Brit. Ceram. Proc.* **39** (1987) 155.
21. S. A. HORTON, D. DOWSON, F. L. RILEY and N. WALLBRIDGE, *Rev. Chimie Minérale* **22** (1985) 576.
22. E. P. ABRAHAMSON II, S. JAHANMIR and N. P. SUH, *Ann. CIRP* **24** (1975) 513.
23. K. KUWAHARA and H. MASUMOTO, *J. Jpn Soc. Lubr. Eng.* February (1980); Abstract in *Lubr. Engng* **36** (1980) 362.

Received 5 April
and accepted 4 September 1989